Research Report

A Fractal-based Flame Propagation Model for Large Eddy Simulation

Hidemasa Kosaka, Yoshihiro Nomura, Makoto Nagaoka, Masahide Inagaki and Masato Kubota

Report received on Mar. 2, 2012

ABSTRACT A novel combustion model for large-eddy simulation (LES) for gasoline engines has been developed. Unlike conventional models based on Reynolds-averaged Navier-Stokes (RANS) models, the new model takes a unique approach; it is described by the fractal characteristics of flame front and a universal expression for the subgrid scale (SGS) flame speed. The present fractal combustion model is applied to calculations of a spark ignition engine. Both the 0-10% and 10-90% combustion periods agree well with the experimental data. Because the modeling of the SGS turbulent speed is based on fractal analysis with experimental observations, the SGS combustion model is able to apply a wide range of engine operating conditions. The present model was applied to a multi-cycle simulation of a single-cylinder engine. The fluctuations at the instant when the heat release rate peaked were compared with data that was obtained experimentally. The calculated magnitude of the fluctuations was found to be close to the experimental values. It is thought that the flow variation generated during the intake stroke significantly influences the cyclic variations.

KEYWORDS Gasoline Engine, Combustion, LES, Numerical Analysis, Modeling, Cyclic Variation

1. Introduction

Computational fluid dynamics (CFD) has developed considerably over the decades, and is now an indispensable tool for analyzing the phenomena that occur in an engine cylinder. While CFD was first used only for flow analysis, it is now also applied to fuel spray, mixture formation and combustion analysis. The numerical analysis methodologies that can be frequently applied to such a turbulent flow are Reynolds averaged Navier-Stokes (RANS) model, large eddy simulation (LES), and direct numerical simulation (DNS). The RANS method is currently adopted as the standard. Although RANS is able to predict only averaged values, its computational cost is relatively low and the usual engineering demand is for an ensemble-averaged characteristics. It is likely to remain useful for some time. It has been pointed out, however, that the flow calculation with the RANS model is not sufficiently accurate. The wrinkled flame sheet observed in experiments cannot be represented by the RANS model and detailed analysis of the flame is difficult. Because the model produces ensemble-averaged value, additional modeling is needed to analyze cyclic variations.

On the other hand, LES, in which large scale of turbulent flow structures are explicitly computed and the effects of the smaller structures are described through the use of a subgrid scale (SGS) model, is a very promising approach for numerically simulating engine combustion,[1] and it has been reported that the prediction accuracy for the flow field is better than with the RANS models.[2-4] It should be possible to directly reproduce the flame development process, detailed flame front,[5] and the cyclic variation by applying LES to the combustion phenomenon.

Experimental evidence indicates that the greatest effect of turbulence is to wrinkle the flame. Namely, a very thin but highly wrinkled flame involving a spectrum of length scales ranging from 0.1 to 1.0 mm is observed, which is smaller than the typical grid width used in the calculations. The flame sheet and the structure cannot be completely resolved with a computational grid so that it is necessary to model this SGS effect to calculate the premixed flame with LES.

The same combustion model expression as that formulated in RANS[6-9] has been most frequently used, even for LES.[10,11] For example, the following

The final, definitive version of this paper has been published in Int. J. Engine Res., Vol.12, Issue 4, August 2011, pp.393-401, by SAGE Publications, Ltd., All rights reserved. © 2011 Institution of Mechanical Engineers.

expression used in the SGS modeling is based on the equation for the averaged turbulent flame speed, with the assumption of Damkohler.

$$\frac{S_T^{SGS}}{S_L} = 1 + C \cdot \left(\frac{u'_{SGS}}{S_L} \right)^n \quad \cdots\cdots\cdots\cdots\cdots\cdots (1)$$

In RANS modeling, S_T^{SGS} and u'_{SGS} are replaced with the mean turbulent flame speed and mean turbulent intensity, respectively, and S_L is the laminar flame speed. Since the mean turbulent flame speed is formulated based on a steady flame speed for the burner flame, it predicts the excessive flame speed in the early combustion stages. The incorporation of the transition time τ from laminar to turbulent flame[12] is usually necessary for RANS calculations:

$$\frac{S_T}{S_{T0}} = \left\{ 1 + \frac{\tau}{\Delta t} \left(\exp\left(\frac{\Delta t}{\tau} \right) - 1 \right) \right\}. \quad \cdots\cdots\cdots\cdots (2)$$

The combustion model for RANS represents the effects of turbulent fluctuations on the mean fields, while the model for LES accounts for the effects of SGS components on the grid scales. The validity of Eqs. 1 and 2 cannot be guaranteed as a SGS combustion model for LES.

In this paper, at first, it will be described to analyze of the SGS combustion characteristics, and then to propose a new model based on the fractal properties of flame sheet. Then, the model will be validated by comparing the flame speed and the cyclic variation with the measurements.

2. Analysis and Modeling of SGS Characteristics

2. 1 Analysis of Flame Structure

Flame front images obtained by LIF indicate that the premixed flame in the engine cylinder is considered as a wrinkled laminar flame as shown in **Fig. 1**.[13] **Table 1** shows the outline of specifications and operating conditions.

Using fractal analysis, the ratio of the turbulent to laminar flame speed is given as follows:[13]

$$\frac{S_T}{S_L} = \frac{A_T}{A_L} = \frac{A_T}{4\pi R^2} = \left(\frac{L_o}{L_i} \right)^{D-2}, \quad \cdots\cdots\cdots\cdots (3)$$

where R is the mean radius of a spherical flame, L_o and L_i are the outer and inner cutoff scales corresponding to the maximum and minimum flame wrinkling size, respectively, and D is the fractal dimension. Δ of the grid size is used to perform a division into two parts to apply this expression to LES, as follows:

$$\frac{S_T}{S_L} = \left(\frac{L_o}{L_i} \right)^{D-2} = \left(\frac{L_o}{\Delta} \right)^{D-2} \left(\frac{\Delta}{L_i} \right)^{D-2}. \quad \cdots\cdots\cdots (4)$$

$(L_o/\Delta)^{D-2}$ shows the behavior of a larger scale than the computational grid which is directly computed in LES. $(\Delta/L_i)^{D-2}$ shows a subgrid scale element that is smaller than the computational grid width. The SGS turbulent flame speed is defined using the latter part as follows:

$$\frac{S_T^{SGS}}{S_L} = \left(\frac{\Delta}{L_i} \right)^{D-2}. \quad \cdots\cdots\cdots\cdots\cdots\cdots (5)$$

Fractal analysis based on the LIF image has been done for the turbulent flame speed S_T/S_L and SGS flame speed S_T^{SGS}/S_L.[13] **Figure 2** shows S_T/S_L and S_T^{SGS}/S_L with the flame propagation at engine speeds of 650 rpm and 1200 rpm.

The turbulent flame speed in the subgrid scale is almost constant, while the turbulent flame speed increases along with the flame propagation. This is because the inner cutoff, fractal dimension, and the

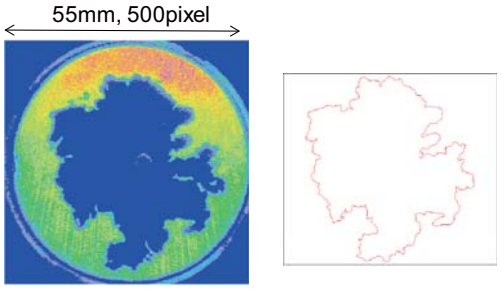

Fig. 1 Example of flame front image obtained by LIF.[13]

Table 1 Engine specifications and operating conditions.

Bore × Stroke	86mm × 86mm
Equivalence Ratio	1.0
Fuel	i-octane
Speed(rpm),Load(%)	1200,50

grid size are almost constant within the combustion period.[13] This trend is same with various equivalence ratios.[13] These results mean that the scale of flame wrinkling hardly changes within combustion period. The outer cutoff scale is almost same as the flame mean radius, while S_T/S_L increases together with the flame propagation.

It can be assumed that the SGS flame speed does not need the transition time from the laminar flame speed to the turbulent flame speed, unlike in RANS. The additional term is required as shown by Eq. 2 for modeling the gradual increase in the turbulent flame speed in RANS.

Fractal analysis based on the data obtained experimentally indicates that it is not reasonable to apply the combustion model formulated for RANS to LES simulation. The development of the flame is governed by the large scale, while the flame development caused by the subgrid scale can be modeled with a universal expression.

2. 2 SGS Combustion Model

It is need to model the inner cutoff L_i to employ the expression given by Eq. 5 for the SGS turbulent flame speed S_T^{SGS} in LES simulation. It is assumed that the inner cutoff L_i is eight times the Kolmogorov scale η :[14]

$$L_i = 8\eta \quad \eta = \left(\frac{\nu^3}{\varepsilon}\right)^{1/4}, \qquad \cdots\cdots\cdots\cdots\cdots\cdots (6)$$

where η is the Kolmogorov scale, ν is the kinetic viscosity, and ε is the dissipation rate of the turbulent energy. It is difficult to calculate ε in LES because it is a statistical value. It is also assumed that the dissipation rate ε is equal to the dissipation rate of SGS turbulent energy ε_{SGS}:[14]

$$\varepsilon \cong \varepsilon_{SGS} = C_\varepsilon \cdot \frac{k_{SGS}^{3/2}}{\Delta}, \qquad \cdots\cdots\cdots\cdots\cdots\cdots (7)$$

where k_{SGS} is the SGS turbulence energy, and C_ε is set to 1.0. As a result, the SGS turbulent flame speed can be modeled as follows:

$$\frac{S_T^{SGS}}{S_L} = \left(\frac{\Delta}{L_i}\right)^{D-2} = C \cdot \left(\frac{\Delta^3 k_{SGS}^{3/2}}{\nu^3}\right)^{(D-2)/4}. \qquad \cdots\cdots (8)$$

D is adjusted to represent the heat release rate of experiments in this paper.

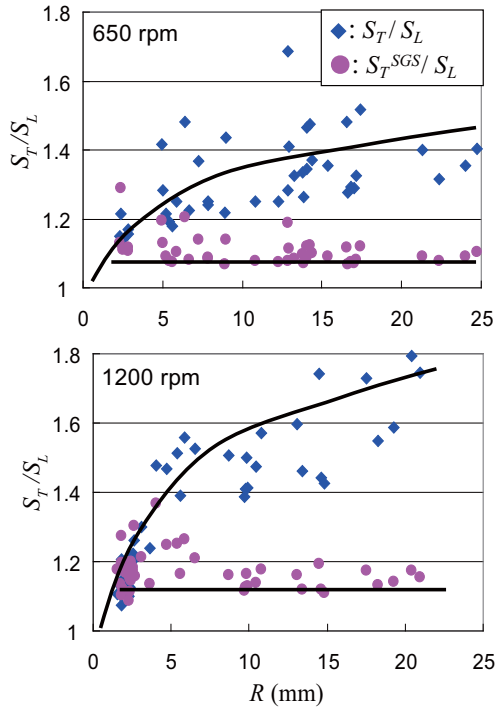

Fig. 2 Turbulent flame speed as a function of a mean flame radius R.

3. Computational Investigations

3. 1 Governing Equations

The governing equations for flow in an engine cylinder are the filtered equations of mass, momentum, and the conservation of energy.

$$\frac{\partial \bar{\rho}}{\partial t} + \frac{\partial}{\partial x_i}\left(\bar{\rho}\tilde{u}_i\right) = 0 \qquad \cdots\cdots\cdots\cdots\cdots\cdots (9)$$

$$\frac{\partial \bar{\rho}\tilde{u}_i}{\partial t} + \frac{\partial}{\partial x_i}\left(\bar{\rho}\tilde{u}_i\tilde{u}_j\right) = -\frac{\partial \bar{p}}{\partial x_j} + \frac{\partial}{\partial x_i}\left\{2\mu\left(\tilde{S}_{ij} - \frac{1}{3}\tilde{S}_{ij}\delta_{ij}\right) - \tau_{ij}\right\} \qquad \cdots\cdots\cdots\cdots (10)$$

$$\tau_{ij} = \bar{\rho}\left(\tilde{u}_i u_j - \tilde{u}_i\tilde{u}_j\right) \; S_{ij} = \frac{1}{2}\left(\frac{\partial \tilde{u}_i}{\partial x_j} + \frac{\partial \tilde{u}_j}{\partial x_i}\right) \qquad \cdots\cdots\cdots\cdots (11)$$

$$C_p\left(\frac{\partial\bar{\rho}\tilde{T}}{\partial t}+\frac{\partial\bar{\rho}\tilde{u}_i\tilde{T}}{\partial x_i}\right)=\frac{\partial}{\partial x_i}\left\{\frac{\mu}{\mathrm{Pr}}\frac{\partial\tilde{T}}{\partial x_i}-q_i^{uT}\right\}+Q \quad \cdots\cdots\cdots\cdots (12)$$

The SGS stress τ_{ij} is modeled using the standard Smagorinsky model,[15] which is one of the most widely used SGS models. The Smagorinsky coefficient C_s has to be adjusted according to the flow configuration, with the value being set to 0.1 in this paper.

$$\tau_{ij}=-2\mu_{SGS}\left(\tilde{S}_{ij}-\frac{1}{3}\tilde{S}_{ij}\delta_{ij}\right) \cdots\cdots\cdots\cdots (13)$$

$$\mu_{SGS}=\bar{\rho}\left(C_S\Delta\right)^2\left(2\tilde{S}_{ij}\tilde{S}_{ij}\right)^{\frac{1}{2}} \cdots\cdots\cdots\cdots (14)$$

$$k_{SGS}=C_k\Delta^2\left(\tilde{S}_{ij}\tilde{S}_{ij}\right) \cdots\cdots\cdots\cdots (15)$$

The SGS heat flux in Eq. 12 is given by assuming SGS Prandtl number as follows:

$$q_i^{uT}=-\frac{\mu_{SGS}}{\mathrm{Pr}_{SGS}}\frac{\partial\tilde{T}}{\partial x_i} \quad \mathrm{Pr}_{SGS}=1.0\ . \cdots\cdots\cdots (16)$$

The conservation of mixture fraction and the progress variable based on the flamelet concept are used to express the premixed and diffusion combustion.

$$\frac{\partial\bar{\rho}\tilde{\xi}}{\partial t}+\frac{\partial\bar{\rho}\tilde{u}_i\tilde{\xi}}{\partial x_i}=\frac{\partial}{\partial x_i}\left\{\frac{\mu}{Sc}\frac{\partial\tilde{\xi}}{\partial x_i}-\eta_i^{u\xi}\right\} \cdots\cdots\cdots (17)$$

$$\eta_i^{u\xi}=\bar{\rho}\left(\xi\tilde{u}_i-\tilde{\xi}\tilde{u}_i\right) \cdots\cdots\cdots\cdots (18)$$

$$\frac{\partial\bar{\rho}\tilde{Y}}{\partial t}+\frac{\partial\bar{\rho}\tilde{u}\tilde{Y}}{\partial x}=\frac{\partial}{\partial x}\left(\frac{\mu_{SGS}}{\sigma_Y}\frac{\partial\tilde{Y}}{\partial x}\right)=-\overline{\rho_u S_L\xi\left|\nabla Y\right|} \cdots\cdots\cdots\cdots (19)$$

$$\overline{\rho_u S_L\xi\left|\nabla Y\right|}=\bar{\rho}S_T{}^{SGS}\left|\nabla\tilde{Y}\right| \cdots\cdots\cdots\cdots (20)$$

The SGS flux term in Eq. 17 is also given by assuming the SGS Schmidt number as follows: [16,17]

$$\eta_i^{u\xi}=-\frac{\mu_{SGS}}{Sc_{SGS}}\frac{\partial\tilde{\xi}}{\partial x_i} \quad Sc_{SGS}=1.0\ . \cdots\cdots\cdots (21)$$

3. 3 Computational Domain and Mesh

Simulations are performed by incorporating the SGS combustion model into STAR-CD, a commercial CFD code. The implicit scheme is employed for temporal discretization. The PISO scheme is used as the solver for the velocity and pressure coupling. The wall function is applied to wall boundary conditions.

Figure 3 presents the computational domain that consists only of the cylinder. The computational mesh consists of 78,440 cells, and the maximum grid size is 0.5mm, which is almost same as the initial flame radius in calculation. The numerical integration time step is imposed by various stability criteria, and is in the order of 0.2 degrees except combustion period. In the combustion period, the numerical time step is in the order of 0.05 degrees to stabilize.

The calculations pertain to the combustion stroke, from the instant that the intake valve closes to the instant that the exhaust valve opens. The treatment of the initial conditions when the intake valve is closed is such that the calculation of the intake flow is performed with another computational grid consisting of the cylinder, intake port, and exhaust port. The calculation result at –150 deg. ATDC, when the intake valve is closed, expanded in the domain consisting of only the cylinder for combustion calculation.

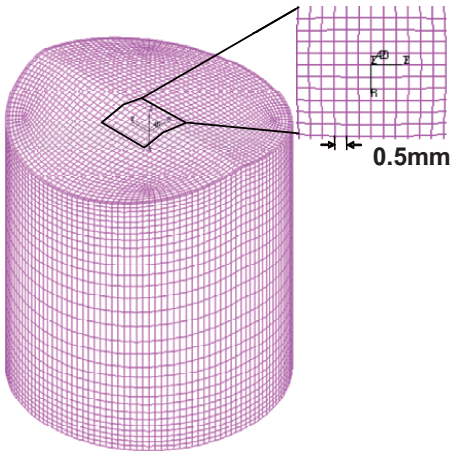

Fig. 3 Computational grid for the combustion stroke (78,440 cells).

4. Model Validations

4. 1 Flame Speed

The flame speed is an extremely important factor in calculation of engine combustion performance, including the combustion period, thus it is important to validate the SGS combustion model for calculating the turbulent flame speed.

Table 2 shows the engine specifications and operating conditions used to obtain data for validating the flame speed for homogeneous premixed combustion. The test engine has a single cylinder with four valves and operates under a range of speeds and load conditions.

Figure 4 is a horizontal section of the temperature distribution from LES and RANS simulations with the same grid for the combustion stroke, –10 deg. ATDC, TDC, and +10 deg. ATDC. It should be noted that the LES-simulated flame structure presents a wrinkle shape like that obtained in the LIF experiments.

Figure 5 compares the pressure histories and heat release rates from the calculated and measured data over a range of engine speeds from 1000 rpm to 4000 rpm. The arrows in Fig. 5 show the ignition timings at which, a flame kernel of 0.5 mm diameter is given at the spark plug in the calculation, and the spark signal is generated in the experiment respectively. In this paper, the ignition timings in the calculation are adjusted to represent the early stage of combustion in the experiments. The heat release rates calculated by the present model give close agreement with the experimental data, though the ignition timings and the fractal dimension are adjusted to reproduce the experimental results.

Figure 6 shows the 0-10% and 10-90% combustion periods, obtained both by calculation and experiment. The measured data used for comparison with the calculated results are average values obtained over

Table 2 Engine specifications and operating conditions.

Bore × Stroke	86mm × 86mm
Equivalence Ratio	1.0
Fuel	n-heptane
Speed(rpm),Load(%)	1000,50
	2000,50
	4000,50

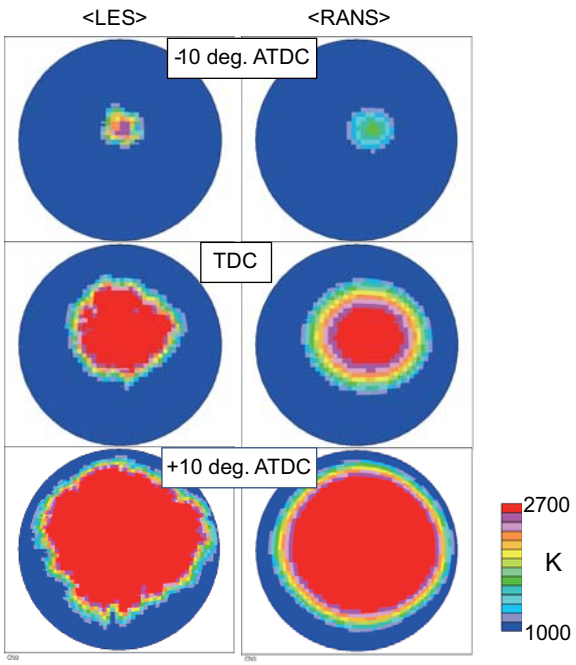

Fig. 4 Horizontal sections of the temperature distribution from LES and RANS simulations.

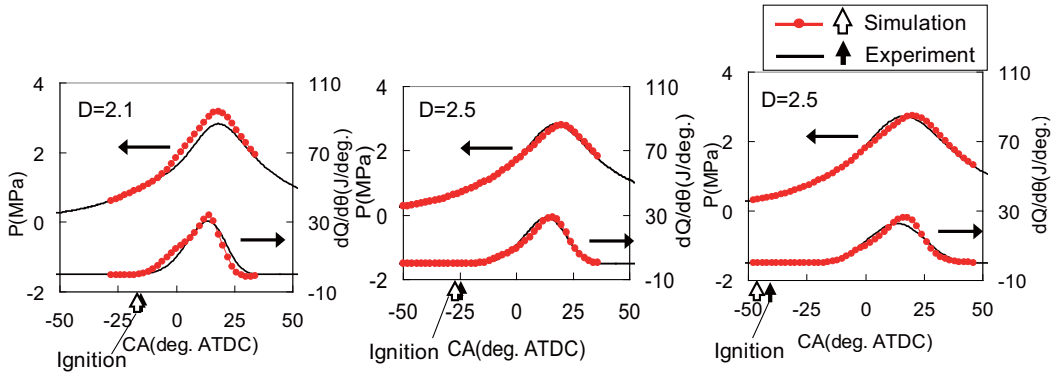

(a) Ne = 1000 rpm (b) Ne = 2000 rpm (c) Ne = 4000 rpm

Fig. 5 Pressure and heat release rate by experiments and LES calculations.

200 cycles. The comparisons of the calculated combustion periods at different engine speeds also indicates that the present model represent the flame speed at a wide range of engine operating conditions.

4. 2 Cyclic Variations

Cyclic variations in combustion process are an important issue in the engine development. Engine operation control parameters such as the optimal spark timing are usually set according to the cycle-averaged characteristics. Fast burning cycles have over-advanced spark timings while, for cycles with a slower combustion process, the timing is retarded. Both lead to reduce the thermal efficiency. This condition is greatly influenced by the flow generated by the intake stroke, which is determined by the shape of the intake port and the design of both the intake valve and the combustion chamber. LES provides the ability to predict cyclic variations because smaller spatial scales and temporal fluctuations can be resolved. Cyclic variations in the turbulent gas motion in SI engines are focused.

4. 2. 1 Numerical and Experimental Setup

Table 3 overviews the calculation of cyclic variations. The computational grid with the intake and exhaust ports is used without the combustion model, to calculate the cyclic variations in the flow generated during the intake stroke. The pressure boundary condition at the end of intake pipe is set to 0.1 MPa. The turbulence at the intake port is generated during several cycle calculations without the combustion model.

The calculated intake flow velocity at –60 deg. ATDC for each cycle is expanded to the computational grid for the combustion simulation as shown in Table 3.

The test engine specification is almost the same as that described in Table 2, with an engine speed of 1200 rpm, the throttle set to WOT, and an ignition timing of –20 deg. ATDC.

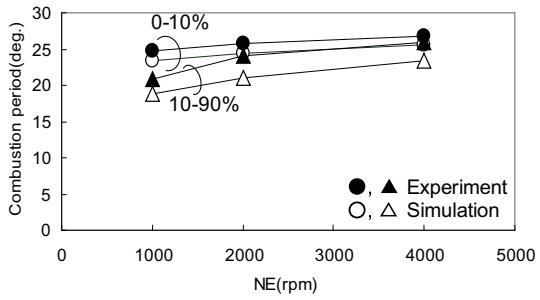

Fig. 6 Relationship between engine speed and combustion period.

Table 3 The overview of the calculation of cyclic variations.

	Cycle=0	Cycle=1	Cycle=2
Cold flow (Motoring)	IVO → Compression → IVC → Expansion	IVO → Compression → IVC → Expansion	IVO → IVC …
Combustion		Combustion	Combustion

4. 2. 2 Results and Discussion

The cold flow was simulated over seven cycles to obtain the initial conditions for the validation of cyclic variations. **Figures 7** and **8** show, for two cycles, the instantaneous field of velocity in a vertical cross-

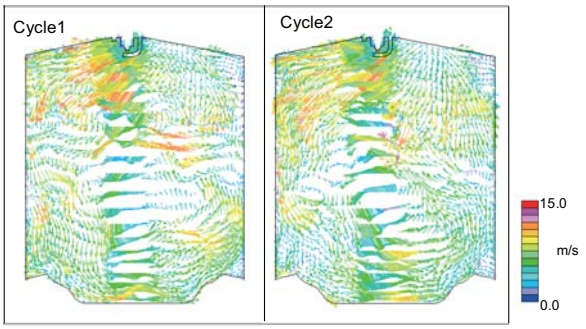

Fig. 7 Comparison of gas velocity distribution (Ne = 1200 rpm, CA = –150 deg. ATDC; intake valve closing).

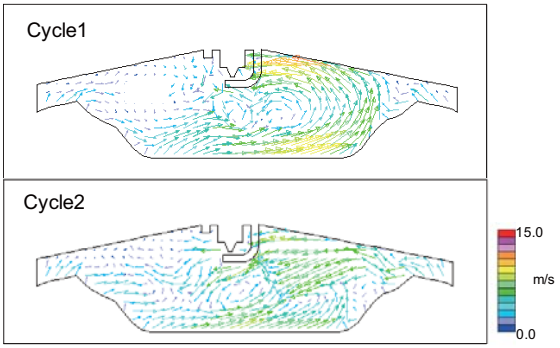

Fig. 8 Comparison of gas velocity distribution (Ne = 1200 rpm, CA = –5 deg. ATDC; ignition).

section at the intake valve closed and ignition, respectively. It can be seen that similar weak tumble flows are formed in each cycle. There are many differences in the fine vortex, even when the intake valve is closed, and these differences lead to the variation in flow velocity near the spark plug at the ignition timing.

Figures 9 and **10** show the instantaneous temperature distributions in a vertical cross-section at the initial stage of combustion and the peak heat release rate in each cycle. **Figure 11** shows the heat release rate obtained from seven computed cycles. The standard deviation for the peak timing of the heat release rate is compared with that obtained experimentally to validate the cyclic variations in the calculation as shown in **Fig. 12**. The magnitude of the standard deviation obtained by simulation is close to that obtained by the experiment. It can be assumed that the difference in the flow field from the intake stroke is one of the main factors affecting cyclic variation for a port-injection gasoline engine operating under WOT conditions. The residual gas distribution is also a major factor under low load or lean conditions.

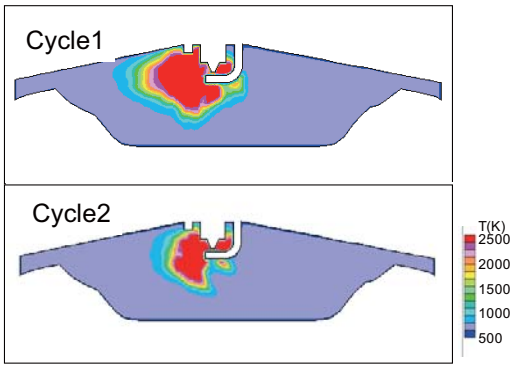

Fig. 9 Comparison of temperature distribution (CA= –8 deg. ATDC; initial stage of combustion).

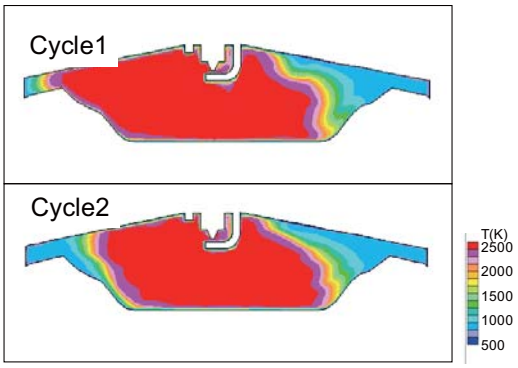

Fig. 10 Comparison of temperature distribution (CA = 10 deg. ATDC; peak of heat release rate).

5. Summaries

A SGS combustion model has been developed from the fractal characteristics of flame front and the inner cutoff expression, in line with the DNS results. The combustion periods calculated by the present model agree well with the experimental data when applied to the phenomenon in the engine cylinder. These results suggest that the flame propagation model based on fractal analysis is an effective approach, though in this study the ignition timings and the model constants are adjusted to reproduce the experimental results. Future work on modeling the flame kernel growth and the universality of model constant is expected to eliminate the ambiguity of the present modeling.

This combustion model has been applied to the multi-cycle simulation of a single-cylinder engine. The fluctuations in time at the peak heat release rate were compared. The same degree of fluctuation as that observed in the experiment was reproduced. It can be

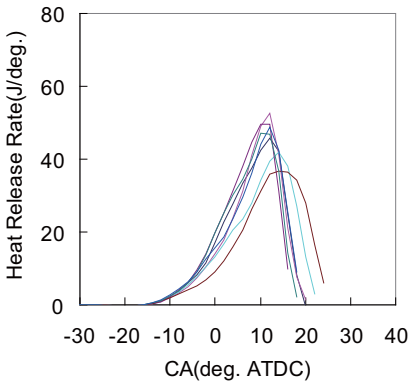

Fig. 11 Heat release rate at different cycle (7 cycles).

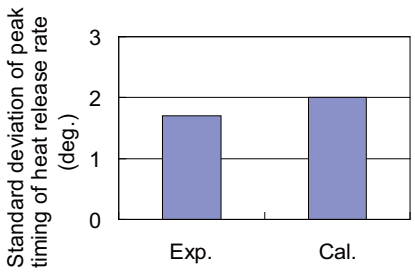

Fig. 12 Cyclic variation range of heat release rate.

assumed that the flow variation generated during the intake stroke has a significant influence on the cyclic variations.

References

(1) Verzicco, R., Mohd-Yusof, J., Orlandi, P. and Haworth, D., "LES in Complex Geometries using Boundary Body Forces", *Proceedings of the Center for Turbulent Research Summer Program 1998* (1998), pp.171-186.

(2) Inagaki, M., Nagaoka, M., Horinouchi, N. and Suga, K., "LES Analysis of Engine Steady Intake Flows Using a Mixed-time-scale SGS Model (in Japanese)", *Trans. of the JSME B*, Vol.73, No.725 (2007), pp.58-66.

(3) Haworth, D. C., "Large-eddy Simulation of In-cylinder Flows", *Oil & Gas Science and Technology -Revue de l Institut Francais du Petrole*, Vol.54, No.2 (1999), pp.175-185.

(4) Tobois, L., Rymer, G., Souleres, T., Poinsot, T. and Van den Heuvel, B., "Large-eddy Simulation for the Prediction of Aerodynamics in IC Engines", *International Journal of Vehicle Design*, Vol.39, No.4 (2005), pp.368-382.

(5) Saijyo, K., Nishiwaki, K. and Yoshihara, Y., "Numerical Analysis of the Interaction between Thermo-fluid Dynamics and Auto-ignition Reaction in Spark Ignition Engines", *JSME International Journal Series B*, Vol.46, No.1 (2003), pp.44-51.

(6) Nomura,Y., Miyagawa, H., Fujikawa, T., Tomoda, T., Kubota, M. and Abe, S., "Numerical Study of Mixture Formation and Combustion Process in a Direct Injection Gasoline Engine with Fan-shaped Spray", *SAE Tech. Pap. Ser.* No.2001-01-0738 (2001).

(7) Bray, K. N. C., Libby, P. A. and Moss, J. B., "Unified Modeling Approach for Premixed Turbulent Combustion I. General Formulation", *Combustion and Flame*, Vol.61, No.1 (1985), pp.87-102.

(8) Meneveau, C. and Poinsot, T., "Stretching and Quenching of Flamelets in Premixed Turbulent Combustion", *Combustion and Flame*, Vol.86, No.4 (1991), pp.311-332.

(9) Boudier, P., Henriot, S., Poinsot, T. and Baritaud, T., "A Model for Turbulent Flame Ignition and Propagation in Spark Ignition Engine", *Proceedings of the Twenty-Fourth Symposium on Combustion* Vol.24, No.1 (1992), pp.503-510.

(10) Flohr, P. and Pitsch, H., "A Turbulent Flame Speed Closure Model for LES of Industrial Burner Flows", *Proceedings of the Center for Turbulent Research Summer Program 2000* (2000), pp.169-179.

(11) Hong, G. I., Thomas, S. L. and Joel, H. F., "Large Eddy Simulation of Turbulent Front Propagation with Dynamic Subgrid Models", *Physics of Fluids*, Vol.9 (1997), pp.3826-3834.

(12) Lipatnikov, A. N. and Chomiak, J., "Modeling of Turbulent Scalar Transport in Expanding Spherical Flames", *SAE Tech. Pap. Ser.* No.2005-01-2109 (2005).

(13) Nomura, Y. and Shimizu, R., "Fractal Analysis of Flame Front during the Early Stages of Propagation in a SI Engine", *Eighteenth Internal Combustion Engine Symp.* (2005).

(14) Shiwaku, N., Nada, Y. and Tanahashi, M., "SGS Modeling of Hierarchical Structures in Turbulent Premixed Fames for Large Eddy Simulation (in Japanese)", *Proceedings of Thermal Engineering Conference 2005* (2005), pp.81-82.

(15) Smagorinsky, J., "General Circulation Experiments with the Primitive Equations, I. The Basic Experiment", *Monthly Weather Review*, Vol.91 (1963), pp.99-164.

(16) Pierce, C. D. and Moin, P., "Progress-variable Approach for Large-eddy Simulation of Non-premixed Turbulent Combustion", *Journal of Fluid of Mechanics*, Vol.504 (2004), pp.73-97.

(17) Bray, K., Domingo, P. and Vervisch, L., "Role of Progress Variable in Models for Partially Premixed Turbulent Combustion", *Combustion and Flame*, Vol.141, No.4 (2005), pp.431-437.

Appendix

Notation

A_L	laminar flame surface area
A_T	turbulent flame surface area
C	model constant
C_S	Smagorinsky constant
D	fractal dimension
k_{SGS}	subgrid turbulence energy
L_i	inner cutoff scale
L_o	outer cutoff scale
n	exponential model constant
Pr	Prandtl number
Pr_{SGS}	subgrid Prandtl number
q_i^{uT}	subgrid heat flux
Q	calorific value
S_{ij}	strain rate tensor
Sc	Schmit number
S_L	laminar flame speed
S_T	turbulent flame speed
S_{T0}	turbulent flame speed without transition time
S_T^{SGS}	subgrid turbulent flame speed
T	gas temperature
u_i	gas velocity
u'_{SGS}	subgrid turbulent intensity
Y	progress variable

δ_{ij} Kronecker delta
Δ grid size
Δt time from ignition timing
ε dissipation rate of the turbulent energy
ε_{SGS} subgrid dissipation rate of the turbulent energy
η Kolmogorov scale
η_i diffusion term of mixture fraction
μ molecular viscosity
μ_{SGS} subgrid molecular viscosity
ν kinetic viscosity
ρ gas density
ρ_u unburnt gas density
τ transition time from the laminar flame to the turbulent flame
τ_{ij} subgrid stress tensor
ξ mixture fraction

Hidemasa Kosaka
Research Fields:
- Computational Fluid Dynamics
- Internal Combustion Engine

Academic Societies:
- Society of Automotive Engineers of Japan
- The Japan Society of Mechanical Engineers

Award:
- Incentive Award, Society of Automotive Engineers of Japan, 2011

Yoshihiro Nomura
Research Field:
- Combustion Modeling and Its Application for Gasoline Engines

Academic Degree: Dr. Eng.
Academic Societies:
- The Japan Society of Mechanical Engineers
- Society of Automotive Engineers of Japan

Awards:
- Paper Award, Gas Turbine Society of Japan, 1992
- JSME Medal for Outstanding Paper,, The Japan Society of Mechanical Engineers, 2003

Makoto Nagaoka
Research Fields:
- Computational Fluid Dynamics
- CAE
- Internal Combustion Engine
- Modeling-simulation-optimization Process

Academic Degree: Dr. Eng.
Academic Societies:
- Society of Automotive Engineers of Japan
- The Japan Society of Mechanical Engineers
- Institute for Liquid Atomization and Spray Systems-Japan

Awards:
- Outstanding Technical Paper Award, Society of Automotive Engineers of Japan, 1992
- SAE Arch T. Colwell Merit Award, 1996
- Incentive Award, The Japan Society of Mechanical Engineers, 1997

Masahide Inagaki
Research Fields:
- Analysis of Heat and Mass Transfer in Manufacturing Process and Cooling System
- Computational Fluid Dynamics

Academic Degree: Dr. Eng.
Academic Societies:
- The Japan Society of Mechanical Engineers
- Japan Society of Fluid Mechanics

Awards:
- JSME Medal for Outstanding Paper, The Japan Society of Mechanical Engineers, 2004
- Best Author Award from JSIAM, The Japan Society for Industrial and Applied Mathematics, 2006

Masato Kubota*
Research Field:
- Research and Development of Innovative CAE Technology

Academic Societies:
- The Japan Society of Mechanical Engineers
- Society of Automotive Engineers of Japan

*Toyota Motor Corporation

